RAA 2018 Vol. **18** No. **5**, 56(6pp) doi: 10.1088/1674–4527/18/5/56

http://www.raa-journal.org *http://iopscience.iop.org/raa*

***R**esearch in*
***A**stronomy and*
***A**strophysics*

On the intrinsic shape of the gamma-ray spectrum for *Fermi* blazars

Shi-Ju Kang[1,2], Qingwen Wu[3], Yong-Gang Zheng[4], Yue Yin[1], Jia-Li Song[1], Hang Zou[1], Jian-Chao Feng[5,2], Ai-Jun Dong[5,2], Zhong-Zu Wu[6], Zhi-Bin Zhang[6] and Lin-Hui Wu[3]

[1] School of Electrical Engineering, Liupanshui Normal University, Liupanshui 553004, China; *kangshiju@hust.edu.cn*
[2] Guizhou Provincial Key Laboratory of Radio Astronomy and Data Processing
[3] School of Physics, Huazhong University of Science and Technology, Wuhan 430074, China; *qwwu@hust.edu.cn*
[4] Department of Physics, Yunnan Normal University, Kunming 650092, China; *ynzgy@ynu.edu.cn*
[5] School of Physics and Electronic Science, Guizhou Normal University, Guiyang 550001, China; *fengjc@gznu.edu.cn*
[6] Department of Physics, College of Science, Guizhou University, Guiyang 550025, China

Received 2017 October 10; accepted 2018 February 10

Abstract The curvature of the γ-ray spectrum in blazars may reflect the intrinsic distribution of emitting electrons, which will further give some information on the possible acceleration and cooling processes in the emitting region. The γ-ray spectra of *Fermi* blazars are normally fitted either by a single power-law (PL) or a log-normal (call Logarithmic Parabola, LP) form. The possible reason for this difference is not clear. We statistically explore this issue based on the different observational properties of 1419 *Fermi* blazars in the 3LAC Clean Sample. We find that the γ-ray flux (100 MeV–100 GeV) and variability index follow bimodal distributions for PL and LP blazars, where the γ-ray flux and variability index show a positive correlation. However, the distributions of γ-ray luminosity and redshift follow a unimodal distribution. Our results suggest that the bimodal distribution of γ-ray fluxes for LP and PL blazars may not be intrinsic and all blazars may have an intrinsically curved γ-ray spectrum, and the PL spectrum is just caused by the fitting effect due to less photons.

Key words: galaxies: active — galaxies: jets — gamma rays: galaxies — galaxies: statistics

1 INTRODUCTION

Blazars, including flat-spectrum radio quasars (FSRQs) and BL Lacertae objects (BL Lacs), are the most powerful active galactic nuclei (AGNs) with a relativistic jet orientated at a small viewing angle with respect to the line of sight (Urry & Padovani 1995). Blazars exhibit rapid variability and high luminosity, high and variable polarization, superluminal motions, core-dominated non-thermal continuum and strong γ-ray emissions, etc (Zhang et al. 2002; Abdo et al. 2010b; Gu & Li 2013; Fan et al. 2016a; Wagner & Witzel 1995; Andruchow et al. 2005; Jorstad et al. 2005). The multi-wavelength spectral energy distribution (SED) from radio to γ-ray bands of blazars dominantly comes from non-thermal emission, where the SED normally exhibits a two-hump structure in the $\log\nu - \log\nu F_\nu$ space. Location of the peak for the lower energy bump in the SED, $\nu_{\rm p}^{\rm S}$, for blazars is used to classify the sources as low (LSP, e.g., $\nu_{\rm p}^{\rm S} < 10^{14}$ Hz), intermediate (ISP, e.g., 10^{14} Hz $< \nu_{\rm p}^{\rm S} < 10^{15}$ Hz) and high-synchrotron-peaked (HSP, e.g., $\nu_{\rm p}^{\rm S} > 10^{15}$ Hz) blazars (e.g., Abdo et al. 2010b). BL Lacs show a wide variety of properties (LSP, ISP and HSP), however, almost all FSRQs are LSP blazars.

It is generally acknowledged that the lower-energy hump is normally attributed to the synchrotron emission produced by non-thermal relativistic electrons in the jet (Urry 1998), but the origin of the second hump is still an open issue. In the leptonic model scenarios, the high-energy γ-rays mainly come from inverse Compton scattering of relativistic electrons either on synchrotron photons inside the jet (synchrotron self-Compton pro-

cess; e.g., Maraschi et al. 1992; Bloom & Marscher 1996; Mastichiadis & Kirk 1997; Konopelko et al. 2003) and/or on some other photon populations from outside the jet (external-Compton process, e.g., Dermer et al. 1992; Dermer & Schlickeiser 1993; Sikora et al. 1994; Ghisellini & Madau 1996; Böttcher & Dermer 1998). The hadron model considers that high-energy γ-ray emission originates from the synchrotron radiation process of extremely relativistic protons (Aharonian 2000; Mücke & Protheroe 2001; Mücke et al. 2003; Petropoulou 2014), or the cascade process of proton-proton or proton-photon interactions (e.g., Mannheim & Biermann 1992; Mannheim 1993; Pohl & Schlickeiser 2000; Atoyan & Dermer 2001; Zheng & Kang 2013; Cao & Wang 2014; Yan & Zhang 2015; Zheng et al. 2016).

The third *Fermi* Large Area Telescope (LAT) source catalog (3FGL) is now available (Acero et al. 2015). The 3FGL catalog includes 3033 γ-ray sources: 2192 high-latitude and 841 low-latitude γ-ray sources, where most sources (1717) are classified as blazars (Ackermann et al. 2015). Based on the 3FGL (Acero et al. 2015), the third catalog of AGNs detected by the *Fermi*-LAT (3LAC) is presented (Ackermann et al. 2015). The high-confidence clean sample of the 3LAC (3LAC Clean Sample), using the first four years of *Fermi*-LAT data, lists 1444 γ-ray AGNs (Ackermann et al. 2015), which include 414 FSRQs ($\sim$ 30%), 604 BL Lac objects ($\sim$ 40%), 402 blazar candidates of uncertain type (BCUs, $\sim$ 30%) and 24 non-blazar AGNs ($<$ 2%). It provides a good chance to study the nature of γ-ray emissions of blazars using such a large sample as *Fermi*-LAT blazars. The physical properties of blazars have been extensively researched based on the *Fermi* source catalogs (e.g., Fan et al. 2016a; Lin & Fan 2016; Fan et al. 2016b; Mao et al. 2016; Ghisellini 2016; Xiong & Zhang 2014; Xiong et al. 2015a,b; Lin et al. 2017; Chen et al. 2016; Singal et al. 2012; Singal 2015). The γ-ray spectrum of *Fermi*-LAT blazars in the 3FGL catalog mainly exhibits two different spectral shapes: Logarithmic Parabola (LP) and Power Law (PL) shapes in the γ-ray spectrum. The physical origin of the different γ-ray spectra is still unclear, which may give some hints on the formation mechanisms of the high-energy electron spectrum in the jet (e.g., Landau et al. 1986; Tramacere et al. 2007, 2009; Massaro et al. 2004a; Yan et al. 2013; Chen 2014; Massaro et al. 2006; Paggi et al. 2009; Massaro et al. 2015; Fan et al. 2016a). In this work, we aim to find (only focus on) the observational differences of blazars with LP and PL γ-ray spectra through statistical analyses of the 3LAC Clean Sample. We give some description of the sample selection in Section 2, and the results are shown in Section 3. The discussion and conclusion are presented in Section 4.

2 SAMPLE

The 3LAC Clean Sample lists 1444 γ-ray AGNs (Ackermann et al. 2015) with 414 FSRQs, 604 BL Lac objects, 402 BCU blazars and 24 non-blazar AGNs. We select 1419 *Fermi* blazars from the 3LAC Clean Sample (3C 454.3, fitted with an exponentially cutoff power law, is neglected). In this sample, the spectra of 130 sources are fitted with LP and those of 1289 sources are fitted with PL.

In Table 1, we present the 3FGL *Fermi* names, redshift, optical classifications (BL Lac and FSRQ, or BCUs) and γ-ray spectral shapes (LP and PL) for selected blazars from the 3LAC website version[1]. In addition, we also compile their variability indexes[2] and γ-ray energy fluxes (S_γ, from 100 MeV to 100 GeV obtained by spectral fitting) from the 3FGL. The γ-ray luminosity (L_γ) is calculated with $\nu L_\gamma = 4\pi D_L^2 \nu S_{\gamma,\rm corr}$, where D_L is the luminosity distance[3]. The γ-ray energy fluxes, S_γ, of the PL γ-ray spectrum in the source rest frame are K-corrected with the formula $S_{\gamma,\rm corr} = S_{\gamma,\rm obs}(1+z)^{\alpha-1}$ (e.g., Lin & Fan 2016; Mao et al. 2016), where z is the redshift, α is the spectral index ($\alpha = \Gamma_{\rm ph} - 1$ and α comes from the $\Gamma_{\rm ph}$ values, and $\Gamma_{\rm ph}$ is power-law photon index, where $dN/dE = K(E/E_0)^{-\Gamma}$) (Acero et al. 2015). For the LP type of γ-ray spectrum blazars, the γ-ray flux is calculated using a modified K-correction according to its spectral shape $S_{\gamma,\rm corr} = S_{\gamma,\rm obs}(1+z)^{1-\alpha'-\beta\log(1+z)}$ (see Mao et al. 2016 for the details and references therein), β is the curvature parameter and α' is obtained from fitting the γ-ray spectrum using a log parabola instead of the usual power law, where $dN/dE = K(E/E_0)^{-\alpha'-\beta\log E/E_0}$ (Acero et al. 2015). In this sample, there are 759 sources with measured redshift (109 LP sources and 650 PL sources). The γ-ray luminosities are also listed in Table 1.

3 RESULTS

We present the statistical results in Figures 1 and 2, where the correlations and histograms are shown for both PL and LP blazars. From the correlations of variability

[1] *http://www.asdc.asi.it/fermi3lac/*

[2] Sum of 2 $\times$ log (likelihood) difference between the flux fitted in each time interval and the average flux over the full catalog interval, see table 16 in Acero et al. (2015).

[3] Here, we adopt the cosmological parameters $H_0 = 70\ {\rm km\,s^{-1}\,Mpc^{-1}}$, $\Omega_M = 0.27$, $\Omega_r = 0$ and $\Omega_\Lambda = 0.73$.

Table 1 Description of the Sample

3FGL name	Optical class	Spectral type	z	S_γ	VI	$\log L_\gamma$
(1)	(2)	(3)	(4)	(5)	(6)	(7)
3FGL J0001.2−0748	BL Lac	PL	...	7.82E–12	49.74	...
3FGL J0001.4+2120	FSRQ	LP	1.106	8.07E–12	130.34	46.27
3FGL J0002.2−4152	BCU	PL	...	3.02E–12	56.35	...
3FGL J0003.2−5246	BCU	PL	...	3.01E–12	45.28	...
3FGL J0004.7−4740	FSRQ	PL	0.880	9.19E–12	112.93	46.67
...	...	...	...	...	...	...

Notes: Col. (1) is the 3FGL name; Col. (2) lists the optical class; Col. (3) gives the gamma-ray spectral type; Col. (4) is redshift; Col. (5) gives the energy flux (S_γ erg cm^{-2} s^{-1}); The variability index (VI) is listed in Col. (6); Col. (7) reports the gamma-ray luminosity (L_γ erg s^{-1}) with a measured redshift. (This table is available in its entirety in xls format on *http:www.raa-journal.org/docs/Supp/ms4116table1.xlsx*.)

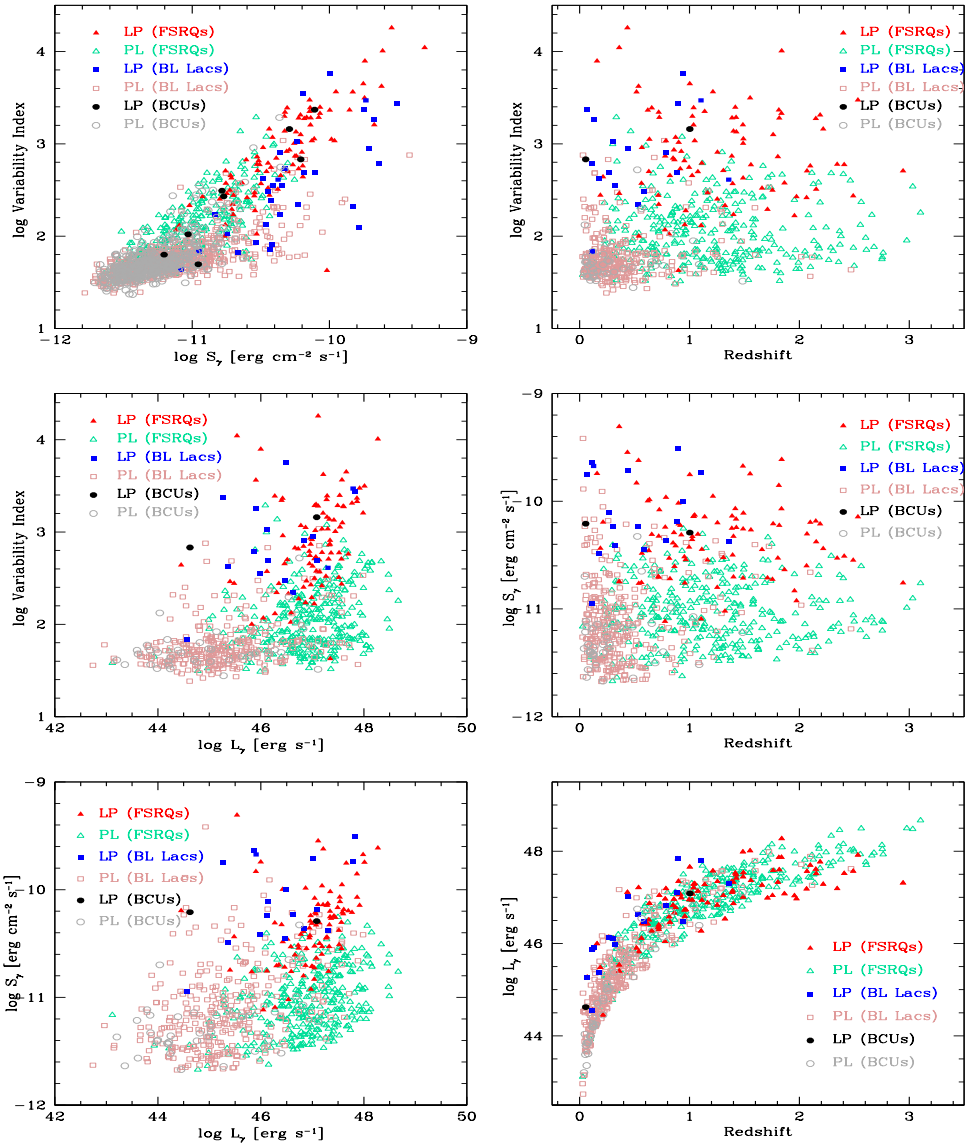

Fig. 1 The correlations between variability index, energy flux (S_γ), gamma-ray luminosity (L_γ) and redshift for blazars. The *red solid triangles*, *blue squares* and *black circles* indicate the observational data for FSRQs, BL Lacs and BCU blazars respectively with the LP-shaped γ-ray spectrum. The *green empty triangles, pink empty squares* and *grey empty circles* represent observational data for FSRQs, BL Lacs and BCU blazars respectively with the PL-shaped γ-ray spectrum.

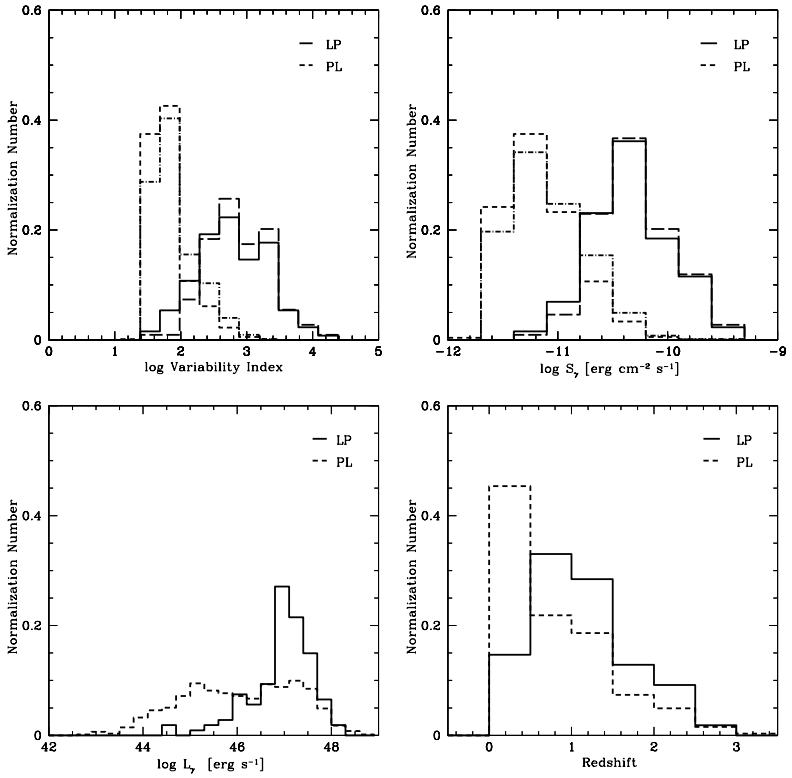

Fig. 2 The normalized histograms for the variability index, γ-ray flux, γ-ray luminosity and redshift for the selected sources, where *solid* and *dashed lines* represent LP and PL shapes of the γ-ray spectrum respectively. In the *upper panels*, the *dot-dashed* and *long-dashed lines* indicate the results for sources with known redshift.

index-S_γ and variability index-L_γ, we find that the LP sources normally have higher γ-ray flux and variability index compared with the PL sources (top left panel of Fig. 1), where the variability index and S_γ show a positive correlation with a Pearson correlations coefficient of 0.81. The histograms of both variability index and γ-ray flux show evident bimodal distributions for LP and PL sources (top panels in Fig. 2), where the KMM-test (see Ashman et al. 1994 for the details and references therein) strongly rejects the hypothesis that LP and PL sources follow a unimodal distribution (probabilities are $1.0 \times 10^{-\infty}$ and 1.25×10^{-33} for variability index and S_γ respectively). The bimodal distributions remain unchanged, even only considering the sources with known redshift (the dot-dashed and long-dashed lines in the top panels in Fig. 2).

From the correlations of variability index-redshift and S_γ-redshift, we find that both LP and PL sources are not well correlated with redshift. The KMM-test also indicates that there is roughly no difference for LP and PL sources in the histogram of redshift, where the probability is $p = 0.995$ (see Table 2), which rejects the bimodal distribution of redshift for these two populations. In the correlations of γ-ray flux-redshift and γ-ray luminosity-redshift, we can find that there are no differences in the distributions of redshift and γ-ray luminosity for LP and PL sources even though LP sources normally have higher fluxes compared with the PL sources. We also show the histogram of γ-ray luminosity for both LP and PL sources in the bottom-right panel of Figure 2, where these two populations should follow a unimodal distribution with a KMM-test probability of $p = 0.999$. In the correlation of γ-ray flux-γ-ray luminosity, we find that the bright sources with higher γ-ray flux show an LP-shaped γ-ray spectrum (e.g. Nolan et al. 2012).

Table 2 Probabilities from the KMM-test

Probabilities	S_γ	VI	z	L_γ
p	$1.0 \times 10^{-\infty}$	1.25×10^{-33}	0.995	0.999

4 DISCUSSION AND CONCLUSIONS

Based on the 3LAC Clean Sample, we compile 1419 *Fermi* blazars with four different parameters: variability index, γ-ray energy flux, γ-ray luminosity and redshift.

We explore the possible differences between LP and PL blazars based on simple statistical analyses of these parameters. We find that the distributions of variability index and γ-ray flux are evidently different for the subsamples of LP and PL blazars (Figs. 1 and 2). However, we do not find evident differences in the distributions of γ-ray luminosity and redshift for LP and PL blazars. Our above conclusions remain unchanged for different optical classes (e.g., for the subsample of BL Lacs and FSRQs), when 402 BCU blazars are excluded.

The unimodal distribution of γ-ray luminosity and bimodal distributions of variability index and γ-ray flux for LP and PL blazars may suggest that these two types of differences may be the effect of observation and the γ-ray spectrum of all sources may be curved if we can detect more γ-ray photons. The γ-ray spectral shape of *Fermi* blazars can shed light on possible intrinsic physics of the jet. For example, the emitting electron energy distribution (EED) can be determined by modeling the SED of blazars (e.g., Landau et al. 1986; Tramacere et al. 2007, 2009; Yan et al. 2013; Cerruti et al. 2013; Kang et al. 2011, 2012; Abdo et al. 2010a; Paggi et al. 2009; Massaro et al. 2004a,b, 2006; Chen 2014). The form of the EED can give further information on the acceleration and cooling processes. First-order Fermi acceleration (shock acceleration) can naturally reproduce the PL EED (e.g., Drury 1983; Drury & Falle 1986; Axford et al. 1977; Drury et al. 1999; Krymskii 1977; Bell 1978a,b; Blandford & Ostriker 1978; Kirk et al. 1998). Second-order Fermi particle acceleration (stochastic acceleration) can form LP EED in the case of the acceleration process dominating over the radiative cooling (e.g., Massaro et al. 2004a,b, 2006; Becker et al. 2006; Tramacere et al. 2011). If there is no acceleration process in the emitting region, the cooled EED is the broken PL shape (e.g., Chiaberge & Ghisellini 1999). Furthermore, it is found that the curvature of the spectrum may be related to the peak frequency of the first hump in the SED of blazars, which seems to support stochastic particle accelerations (e.g., Chen 2014). The intrinsically curved γ-ray spectrum may be induced by the curved EED coming from the stochastic acceleration process, or stochastically dominant acceleration process (e.g., Lewis et al. 2018). It should be noted that extragalactic background light might play a role in the curvature of gamma-ray spectra by altering the intrinsic spectral shape of blazars. This will impact conclusions on the intrinsic particle distribution in blazar jets (e.g., Aleksić et al. 2015).

It is also important to note that the BCU blazars and/or cases without distance information might be biased towards BL Lac objects as the absence of spectral line features is a major hurdle in their identification and distance measurements. It is mandatory to exclude selection effects that can bias the statistical analyses of the parameter spaces, thereby affecting conclusions on the jet physics of the *Fermi*-LAT blazars. The fainter and brighter sets of sources follow broader and more overlapping ranges in luminosity and redshift than they do in their flux. Such analysis would require issues of redshift completeness to be addressed, and the application of sophisticated statistical tools.

In this work, in addition, we merely take a published *Fermi* catalog and make various X-Y and histogram plots, adding no external data, and have not done any of the fittings ourselves. Our results are only based on data obtained from the *Fermi* catalog, for the limited parameters, via a simple statistical analysis (e.g., bimodality test), that explores the intrinsic gamma-ray spectrum of *Fermi* blazars by comparing the LP and PL blazars. The conclusions suggest an obvious inference that the fainter sources could be more complex in their properties — more complex analysis is inhibited by the fact that they are fainter sources. This result could be somewhat biased due to the simple statistical approach, the limited sample and the source of the sample data (obtained from the *Fermi* catalog fitted by the *Fermi* team). A more preferable statistical approach that uses a large and complete sample, more parameters (e.g., mass of the central black hole, and/or polarization information about the jet radiation, etc.) and a sophisticated fitting analysis are needed to further address the intrinsic jet physics of *Fermi*-LAT blazars.

Acknowledgements We thank the anonymous referee for very constructive and helpful comments and suggestions, which greatly helped us to improve our paper. This work is supported by the National Natural Science Foundation of China (Grant Nos. 11763005, 11622324, 11573009, 11763002, U1431111 and U1431126). This work is also supported by the Research Foundation for Advanced Talents of Liupanshui Normal University (LPSSYKYJJ201506), the Open Fund of Guizhou Provincial Key Laboratory of Radio Astronomy and Data Processing, the Physical Electronic Key Discipline of Guizhou Province (ZDXK201535), the Natural Science Foundation of the Department of Education of Guizhou Province (QJHKYZ[2015]455) and the Research Foundation of Liupanshui Normal University (LPSSYDXS1514 and LPSSY201401).

References

Abdo, A. A., Ackermann, M., Agudo, I., et al. 2010a, ApJ, 721, 1425

Abdo, A. A., Ackermann, M., Agudo, I., et al. 2010b, ApJ, 716, 30

Acero, F., Ackermann, M., Ajello, M., et al. 2015, ApJS, 218, 23

Ackermann, M., Ajello, M., Atwood, W. B., et al. 2015, ApJ, 810, 14

Aharonian, F. A. 2000, New Astron., 5, 377

Aleksić, J., Ansoldi, S., Antonelli, L. A., et al. 2015, MNRAS, 450, 4399

Andruchow, I., Romero, G. E., & Cellone, S. A. 2005, A&A, 442, 97

Ashman, K. M., Bird, C. M., & Zepf, S. E. 1994, AJ, 108, 2348

Atoyan, A., & Dermer, C. D. 2001, Physical Review Letters, 87, 221102

Axford, W. I., Leer, E., & Skadron, G. 1977, International Cosmic Ray Conference, 11, 132

Becker, P. A., Le, T., & Dermer, C. D. 2006, ApJ, 647, 539

Bell, A. R. 1978a, MNRAS, 182, 147

Bell, A. R. 1978b, MNRAS, 182, 443

Blandford, R. D., & Ostriker, J. P. 1978, ApJ, 221, L29

Bloom, S. D., & Marscher, A. P. 1996, ApJ, 461, 657

Böttcher, M., & Dermer, C. D. 1998, ApJ, 501, L51

Cao, G., & Wang, J. 2014, ApJ, 783, 108

Cerruti, M., Dermer, C. D., Lott, B., Boisson, C., & Zech, A. 2013, ApJ, 771, L4

Chen, L. 2014, ApJ, 788, 179

Chen, Y.-Y., Zhang, X., Xiong, D.-R., Wang, S.-J., & Yu, X.-L. 2016, RAA (Research in Astronomy and Astrophysics), 16, 13

Chiaberge, M., & Ghisellini, G. 1999, MNRAS, 306, 551

Dermer, C. D., & Schlickeiser, R. 1993, ApJ, 416, 458

Dermer, C. D., Schlickeiser, R., & Mastichiadis, A. 1992, A&A, 256, L27

Drury, L. O. 1983, Reports on Progress in Physics, 46, 973

Drury, L. O., Duffy, P., Eichler, D., & Mastichiadis, A. 1999, A&A, 347, 370

Drury, L. O., & Falle, S. A. E. G. 1986, MNRAS, 223, 353

Fan, J. H., Yang, J. H., Liu, Y., et al. 2016a, ApJS, 226, 20

Fan, X.-L., Bai, J.-M., & Mao, J.-R. 2016b, RAA (Research in Astronomy and Astrophysics), 16, 173

Ghisellini, G. 2016, Galaxies, 4, 36

Ghisellini, G., & Madau, P. 1996, MNRAS, 280, 67

Gu, M. F., & Li, S.-L. 2013, A&A, 554, A51

Jorstad, S. G., Marscher, A. P., Lister, M. L., et al. 2005, AJ, 130, 1418

Kang, S. J., Huang, B. R., Kang, T., Liang, J. H., & Zheng, Y. G. 2011, Acta Astronomica Sinica, 52, 357

Kang, S.-j., Huang, B.-r., Kang, T., Liang, J.-h., & Zheng, Y.-g. 2012, Chinese Astronomy and Astrophysics, 36, 115

Kirk, J. G., Rieger, F. M., & Mastichiadis, A. 1998, A&A, 333, 452

Konopelko, A., Mastichiadis, A., Kirk, J., de Jager, O. C., & Stecker, F. W. 2003, ApJ, 597, 851

Krymskii, G. F. 1977, Soviet Physics Doklady, 22, 327

Landau, R., Golisch, B., Jones, T. J., et al. 1986, ApJ, 308, 78

Lewis, T. R., Finke, J. D., & Becker, P. A. 2018, ApJ, 853, 6

Lin, C., & Fan, J.-H. 2016, RAA (Research in Astronomy and Astrophysics), 16, 103

Lin, C., Fan, J.-H., & Xiao, H.-B. 2017, RAA (Research in Astronomy and Astrophysics), 17, 066

Mannheim, K. 1993, A&A, 269, 67

Mannheim, K., & Biermann, P. L. 1992, A&A, 253, L21

Mao, P., Urry, C. M., Massaro, F., et al. 2016, ApJS, 224, 26

Maraschi, L., Ghisellini, G., & Celotti, A. 1992, ApJ, 397, L5

Massaro, E., Perri, M., Giommi, P., & Nesci, R. 2004a, A&A, 413, 489

Massaro, E., Perri, M., Giommi, P., Nesci, R., & Verrecchia, F. 2004b, A&A, 422, 103

Massaro, E., Tramacere, A., Perri, M., Giommi, P., & Tosti, G. 2006, A&A, 448, 861

Massaro, F., Thompson, D. J., & Ferrara, E. C. 2015, A&A Rev., 24, 2

Mastichiadis, A., & Kirk, J. G. 1997, A&A, 320, 19

Mücke, A., & Protheroe, R. J. 2001, Astroparticle Physics, 15, 121

Mücke, A., Protheroe, R. J., Engel, R., Rachen, J. P., & Stanev, T. 2003, Astroparticle Physics, 18, 593

Nolan, P. L., Abdo, A. A., Ackermann, M., et al. 2012, ApJS, 199, 31

Paggi, A., Massaro, F., Vittorini, V., et al. 2009, A&A, 504, 821

Petropoulou, M. 2014, MNRAS, 442, 3026

Pohl, M., & Schlickeiser, R. 2000, A&A, 354, 395

Sikora, M., Begelman, M. C., & Rees, M. J. 1994, ApJ, 421, 153

Singal, J. 2015, MNRAS, 454, 115

Singal, J., Petrosian, V., & Ajello, M. 2012, ApJ, 753, 45

Tramacere, A., Giommi, P., Perri, M., Verrecchia, F., & Tosti, G. 2009, A&A, 501, 879

Tramacere, A., Massaro, E., & Taylor, A. M. 2011, ApJ, 739, 66

Tramacere, A., Massaro, F., & Cavaliere, A. 2007, A&A, 466, 521

Urry, C. M. 1998, Advances in Space Research, 21, 89

Urry, C. M., & Padovani, P. 1995, PASP, 107, 803

Wagner, S. J., & Witzel, A. 1995, ARA&A, 33, 163

Xiong, D. R., & Zhang, X. 2014, MNRAS, 441, 3375

Xiong, D., Zhang, X., Bai, J., & Zhang, H. 2015a, MNRAS, 451, 2750

Xiong, D., Zhang, X., Bai, J., & Zhang, H. 2015b, MNRAS, 450, 3568

Yan, D., & Zhang, L. 2015, MNRAS, 447, 2810

Yan, D., Zhang, L., Yuan, Q., Fan, Z., & Zeng, H. 2013, ApJ, 765, 122

Zhang, L. Z., Fan, J.-H., & Cheng, K.-S. 2002, PASJ, 54, 159

Zheng, Y. G., & Kang, T. 2013, ApJ, 764, 113

Zheng, Y. G., Yang, C. Y., & Kang, S. J. 2016, A&A, 585, A8